Diatom autofocusing in brightfield microscopy: A comparative study

Conference Paper · February 2000

DOI: 10.1109/ICPR.2000.903548 · Source: IEEE Xplore

4 authors, including:

Jose Luis Pech Pacheco
Neurologyca

Gabriel Cristobal
Spanish National Research Council

Diatom autofocusing in brightfield microscopy: a comparative study

J. L. Pech-Pacheco & G. Cristóbal
Imaging & Vision Dept.
Instituto de Optica (CSIC)
Serrano 121, 28006 Madrid. Spain
{pech,gabriel}@optica.csic.es

J. Chamorro-Martínez & J. Fernández-Valdivia
Depto. Ciencias de la Computación e I.A.
ETS de Ingeniería Informática
Avda. Andalucía, 38, 18071 Granada. Spain
{jesus,J.Fdez-Valdivia}@decsai.ugr.es

Abstract

We present a number autofocusing methods in lightning microscopy for its use in diatom identification. Among these, the Tenengrad method has been considered one of the best. The basic requirements for a practical autofocusing system are speed, sharpness and robustness to noise.Recently other focus measures based on a modified Laplacian method are said to perform better than Tenengrad. We investigate two sound methods based on a modified Tenengrad and a modified Laplacian. Measurements show that provide a reliable and suitable focus measure than other similar methods. We investigate the window size analysis dependency and perform an univariate analysis on the focus measures. The focusing techniques are implemented in an automatic slide scanning system for diatom detection and identification for its use in the ADIAC project. [1]

1. Introduction

Diatoms are unicelular algae related with brown algae that grow anywhere where there exists enough light and moisture. They are ecologically very important because they contribute around the 20% of the world's carbon fixation [3]. Besides the ecological interest, there exists a number of other fields where diatom analysis is useful: geological, climatological, geographical,archeological or forensic research. Many applications diatom analysis require both the presence of experts and the identification of a large range of diatom species and therefore are tedious and time consuming. However, most of the existent computer-based diatom analysis methods do not tackle the whole automatization process [2, 7]. One key aspect in the automatization process is to determine reliable and fast autofocusing methods. Groen et al [4] has identified eight different criteria for comparing autofocus algorithms [4]. Many focusing techniques have been proposed in the literature [5, 9, 10, 6, 1]. Most of them extract a focus measure that gives a maximum for the best focused image. Defocus algorithms be classified into two categories: those based on the statistical variance pixel values and those based on spatial-frequency content of the image. In this paper, we propose new algorithms based on the computation of the variance of the image gradient or image Laplacian that provides sharper focus measures than the pure variance-based or pure spatial-based methods for a similar computational cost.

[1]This work has been supported in part by the following Grants: EU ADIAC MAS3-CT97-0122 and EU INCO-DC AMOVIP 961646 Project

2. Materials and dataset

Different diatom samples from fresh water and human tissue [2] were analyzed with a Zeiss Axiophot photomicroscope illuminated with a 100W halogen light with 40X lenses. For image acquisition, we used a Scion frame grabber that includes the NIH image processing shareware connected to a CCD analog camera from Pulnix. Two PC image analysis systems (Pentium II &III) were used one for image acquisition and the other one for algorithm computation. Furthermore, for computer intensive calculations a SUN Enterprise 450 with four processors was used. Images have been digitized with 8 bit/pixel and 256x256 pixel image format. The microscope slide was moved with a X-Y-Z motorized stage from Prior Instruments, with a step size of 0.1 μm for the X-Y axis and 1 μm for the Z-axis.

Fig. 1 shows some images of strewn slides with many diatoms and other biological debris.

[2]We thank Dr. M. Bayer from Royal Botanical Garden Edinburgh and Dr. B. Ludes from Inst. of Legal Medicine (Univ. Louis Pasteur) for providing us some sample slides of diatoms

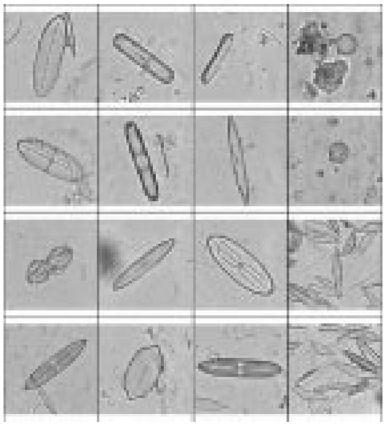

Figure 1. Examples of diatoms with some biological detritus

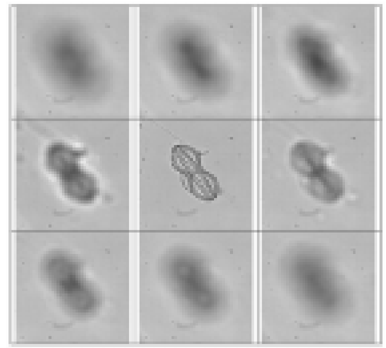

Figure 2. Stack of 9 images at different focus planes

3. Methods

We have evaluated seven focus measures and selected those that perform the best. The criteria used were: (i) Variance (it depends upon the probability distribution and not its spatial distribution); (ii) Entropy (a measure of the histogram uniformity. It fails with images with complicated texture); (iii) Tenengrad (based on Sobel gradient); (iv) Brenner (gradient);(v) Sobel+variance; (vi) Laplacian and (vii) Laplacian+variance. We describe here the variance method (i) and the two proposed methods (v) and (vii).

3.1. Local variance

Let us assume a stack of k images of size MxN taken by changing the microscope focus in steps of 1 μm. Fig. 2 shows some examples of the image stack above and below the best focused image located at the center of the panel. The local variance at point (m,n), m=1,...,M and n=1,...,N is given by:

$$lv_k(m,n) = \frac{1}{w_x w_y} \sum_{i=0}^{w_x} \sum_{j=0}^{w_y} [f_k(m+i,n+j) - \overline{f}_k(m,n)]^2 \tag{1}$$

where $\overline{f}_k$ represents the mean value:

$$\overline{f}_k(m,n) = \frac{1}{w_x w_y} \sum_{i=0}^{w_x} \sum_{i=0}^{w_y} [f_k(m+i,n+j)] \tag{2}$$

$$\tag{3}$$

and the final focus measure, will be given by the global variance of the previous local variance image:

$$fm_k^V = \frac{1}{MN} \sum_{m=0}^{M} \sum_{n=0}^{N} [lv_k(m,n) - \overline{lv}_k(m,n)]^2 \tag{4}$$

where fm_k^V gives the focus measure for the image k and $\overline{lv}_k$ is the global variance value:

$$\bar{l}v_k = \frac{1}{MN} \sum_{m=0}^{M} \sum_{n=0}^{N} [lv_k(m,n)] \tag{5}$$

3.2. Variance of gradient magnitude

The use of image gradients (either the first or second derivatives) are instrumental in order to determine a reliable focus measure. In particular the Tenengrad method is considered as a benchmark in this field. The method is based on computing the gradient magnitude of a Sobel operator:

$$g_k(m,n) = \sqrt{g_x(m,n)^2 + g_y(m,n)^2} \tag{6}$$

where $g_x(m,n)$ and $g_y(m,n)$ are the convolutions with the kernels: $\begin{pmatrix} -1 & 0 & 1 \\ -2 & 0 & 2 \\ -1 & 0 & 1 \end{pmatrix}$ $\begin{pmatrix} 1 & 2 & 1 \\ 0 & 0 & 0 \\ -1 & -2 & -1 \end{pmatrix}$ respectively.
For each image m in the stack, the Tenengrad method provides a focus measure given by:

$$fm_k^G = \sum_m \sum_n [g_k(m,n)]^2 \tag{7}$$

The best focused image will be given by the maximum of fm_k^G.

3.3. Variance of Laplacian magnitude

This technique is similar to gradient magnitude but using a second derivative operator. We use the Laplacian with the convolution kernel:
$\frac{1}{6}\begin{pmatrix} 0 & -1 & 0 \\ -1 & 4 & 1 \\ 0 & -1 & 0 \end{pmatrix}$ The method is based on computing the absolute value of the Laplacian operator.

4. Results

Here we propose a variant of this method based on use the variance of the magnitude of the Sobel gradient. The rationale of this approach is to define a more discriminative measure similar to a second derivative (Laplacian) but increasing the robustness to noise. Fig. 3a,b shows a comparison of focus measurements without and with noise respectively [3].

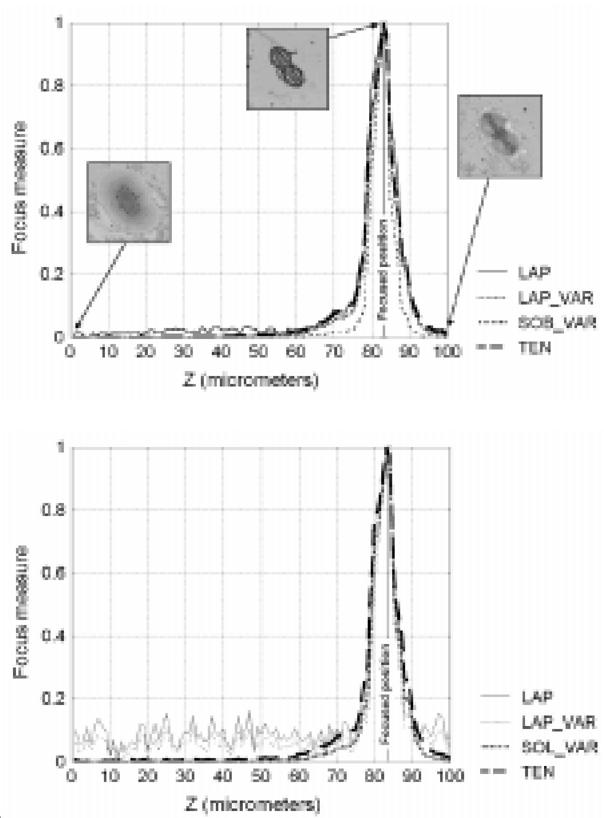

Figure 3. Focus measures (4 methods)

[3]For a subjective focus and image fusion assessment see: http://www.iv.optica.csic.es/projects/autof.html

4.1. Window size selection

Another criteria to take into account is the window size selection for variance and gradient calculation. Fig. 4a shows as a box plot that the variance method provide a better focus estimate for small windows, but with the tradeoff of a higher computational cost than large windows. However, Fig. 4b shows that the Sobel variance provides better results for large windows that leads to a reduction in the computational complexity. Next, we analyze the shape of the focus measures.

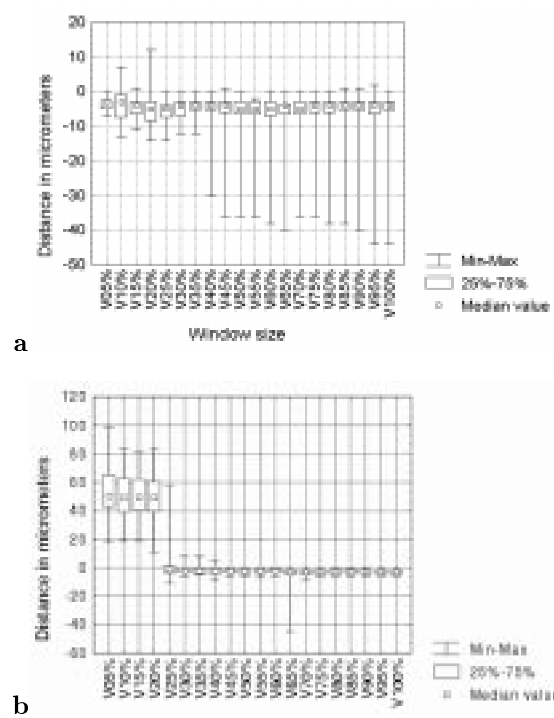

Figure 4. Window size evaluation. (a) Variance measure. (b) Variance of Sobel measure. Horizontal axis gives window size as percentage of the full image size. The zero level corresponds to best focus.

4.2. Focus assessment

• Sharpness. Sharpness is not the only criteria for selecting a good focus measure. In fact, as Subbarao et al [9] has pointed out any focus measure can be artificially sharpened by simply squaring the focus measure. Kurtosis is a candidate for peakedness. However it suffers of a high noise sensitivity. We define an progresive sharpness measure based on the absolute sum of differences of three equidistant focus levels from the maximum value:

$$F_1 = k_1 \sum_{i \neq j} |d_i - d_j| \qquad (8)$$

where d_i and d_j represent the level intersections in the central lobe of the focus measure (Fig. 3b) and k_1 is a normalized constant. Fig. 5 shows that both Sobel+variance and Tenengrad methods provide the sharper focus response (i.e. a smaller F_1 value).

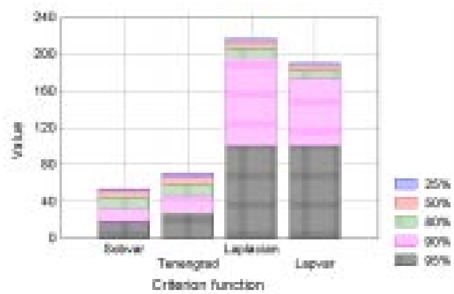

Figure 5. Focus noisy measures peakedness results for four selected methods

- Smoothness and noise sensitivity

We define a relative measure based on an accumulative sum of the absolute gradient value of the focus measure (Fig. 3) with respect to a fitting Gaussian with ($\sigma = 1$).

$$F_2 = \frac{\sum_k |AF'_k|}{\sum_k |AF_k|_G} \qquad (9)$$

where AF'_k represents the first derivative of the focus measure. Next table shows that both Sobel+variance and Tenengrad methods provide the smaller values of F_2 that correspond to a better noise tolerance.

Sobel+var	Tenengrad	Laplacian	Laplacian+var
1.0411	1.0646	2.507	2.101

4.3. Multi-focus fusion techniques

Since diatoms have a 3-D valve we are investigating fusion-based methods for combining different focal planes. We tested several fusion methods and asked to a group of diatom experts about the best result. Fig. 6 shows the fused image selected by the experts from a stack of 8 focus planes. We used a Laplacian pyramid-based method for its calculation [8]. The recombination process produces a contrast enhanced image and the fine diatom striae becomes more visible

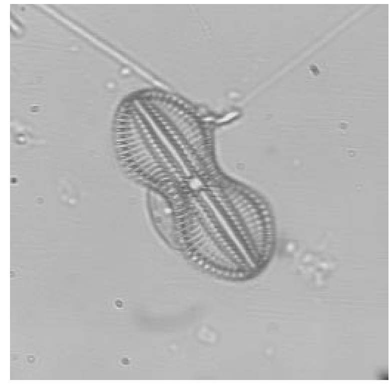

Figure 6. Fused example corresponding to a stack of 8 images

References

[1] W. Bocker, W. Rolf, W. Muller, and C. Streffer. Investigations about autofocus-algorithms for fluorescent-microscopy. In *SPIE Applications of Digital Image Processing XIX*, volume 2847, pages 445–456, Denver, CO, 1996.

[2] J. Cairns, K. Dickson, G. Lanza, S. Almeida, and D. del Balzo. Coherent optical spatial filtering of diatoms in water pollution monitoring. *Archiv. Mikrobiol.*, 83:141–146, 1972.

[3] C. Field, M. Behrenfeld, J. Randerson, and P. Falkowski. Primary production of the biosphere: integrating terrestrial and oceanic components. *Science*, 281:237–240, 1998.

[4] F. Groen, I. Young, and G. Ligthard. A comparison of different focus functions for use in autofocus algorithms. *Cytometry*, 6:81–91, 1985.

[5] E. Krotkov. Focusing. *Int. J. Comp. Vision*, 1:223–237, 1987.

[6] S. K. Nayar and Y. Nakagawa. Shape from focus. *IEEE Trans. on Patt. Anal. and Machine Intell.*, 16(8):824–831, 1994.

[7] J. Pech-Pacheco and J. Alvarez-Borrego. Optical-digital system applied to the identification of five phytoplancton species. *Mar. Biol.*, 132:357–365, 1998.

[8] O. Rockinger. *Multiresolution-Verfahren zur fusion dynamischer bildfolgen.* PhD thesis, Technischen Universitat Berlin, 1999.

[9] M. Subarao and A. Nikzad. Focusing techniques. *Opt. Eng.*, 32(11):2824–2836, 1993.

[10] T. Yeo, S. Ong, Jayasooriah, and R. Sinniah. Autofocusing for tissue microscopy. *Image and Vision Comp.*, 11(10):629–639, 1993.